TU Delft

Delft University of Technology

# Solute transport at the interface of cartilage and subchondral bone plate

## Effect of micro-architecture

Pouran, Behdad; Arbabi, Vahid; Bleys, Ronald L.A.W.; van Weeren, P. Rene; Zadpoor, Amir; Weinans, Harrie

**DOI**
10.1016/j.jbiomech.2016.12.025

**Publication date**
2017

**Document Version**
Final published version

**Published in**
Journal of Biomechanics

**Citation (APA)**
Pouran, B., Arbabi, V., Bleys, R. L. A. W., van Weeren, P. R., Zadpoor, A., & Weinans, H. (2017). Solute transport at the interface of cartilage and subchondral bone plate: Effect of micro-architecture. *Journal of Biomechanics*, *52*, 148-154. https://doi.org/10.1016/j.jbiomech.2016.12.025

**Important note**
To cite this publication, please use the final published version (if applicable).
Please check the document version above.

**Copyright**
Other than for strictly personal use, it is not permitted to download, forward or distribute the text or part of it, without the consent of the author(s) and/or copyright holder(s), unless the work is under an open content license such as Creative Commons.

**Takedown policy**
Please contact us and provide details if you believe this document breaches copyrights.
We will remove access to the work immediately and investigate your claim.

*This work is downloaded from Delft University of Technology.*
*For technical reasons the number of authors shown on this cover page is limited to a maximum of 10.*

Journal of Biomechanics 52 (2017) 148–154

Contents lists available at ScienceDirect

Journal of Biomechanics

journal homepage: www.elsevier.com/locate/jbiomech
www.JBiomech.com

# Solute transport at the interface of cartilage and subchondral bone plate: Effect of micro-architecture

Behdad Pouran [a,b,*], Vahid Arbabi [a,b], Ronald LAW Bleys [c], P. René van Weeren [d], Amir A. Zadpoor [b], Harrie Weinans [a,b,e]

[a] Department of Orthopedics, UMC Utrecht, Heidelberglaan 100, 3584 CX Utrecht, The Netherlands
[b] Department of Biomechanical Engineering, Faculty of Mechanical, Maritime, and Materials Engineering, Delft University of Technology (TU Delft), Mekelweg 2, 2628 CD Delft, The Netherlands
[c] Department of Anatomy, UMC Utrecht, Heidelberglaan 100, 3584 CX Utrecht, The Netherlands
[d] Department of Equine Sciences, Faculty of Veterinary Medicine, University of Utrecht, Yalelaan 112, 3584 CM Utrecht, The Netherlands
[e] Department of Rheumatology, UMC Utrecht, Heidelberglaan 100, 3584 CX Utrecht, The Netherlands

ARTICLE INFO

*Article history:*
Accepted 20 December 2016

*Keywords:*
Osteochondral interface
Micro-computed tomography
Iodixanol diffusion
Subchondral plate thickness and porosity
Articular cartilage
Osteoarthritis

ABSTRACT

Cross-talk of subchondral bone and articular cartilage could be an important aspect in the etiology of osteoarthritis. Previous research has provided some evidence of transport of small molecules (~370 Da) through the calcified cartilage and subchondral bone plate in murine osteoarthritis models. The current study, for the first time, uses a neutral diffusing computed tomography (CT) contrast agent (iodixanol, ~1550 Da) to study the permeability of the osteochondral interface in equine and human samples. Sequential CT monitoring of diffusion after injecting a finite amount of contrast agent solution onto the cartilage surface using a micro-CT showed penetration of the contrast molecules across the cartilage-bone interface. Moreover, diffusion through the cartilage-bone interface was affected by thickness and porosity of the subchondral bone as well as the cartilage thickness in both human and equine samples. Our results revealed that porosity of the subchondral plate contributed more strongly to the diffusion across osteochondral interface compared to other morphological parameters in healthy equine samples. However, thickness of the subchondral plate contributed more strongly to the diffusion in slightly osteoarthritic human samples.

© 2017 Elsevier Ltd. All rights reserved.

## 1. Introduction

Etiology of osteoarthritis (OA) implies deterioration of subchondral bone plate quality such as early thinning, sclerosis and porosity alterations beside the damage of articular cartilage (Pan et al., 2012; Weinans et al., 2012). The severity and type of those changes depend primarily on the OA stage (Botter, 2010; Botter et al., 2011; Intema et al., 2010a; Li and Aspden, 1997). According to some theories that go against conventional theories (Intema et al., 2010b; Sniekers et al., 2008), OA initiates from the subchondral bone, over-time progressing to the overlying articular cartilage (Radin and Rose, 1986; Westacott, 2002). Regardless of whether one subscribes to the conventional or alternative theories associated with the etiology of OA, it is clear that morphological changes in the subchondral bone and articular cartilage create a driving force for transfer of putative harmful molecules (Weinans et al., 2012). Enhanced activity of osteoclasts and subsequent increased subchondral bone perforations and thinning augment the diffusion of cytokines and enzymes as well as cross-talk between cartilage and subchondral bone (Botter et al., 2011; Pan et al., 2009a, 2012; Siebelt et al., 2014). These mechanisms highlight the fact that diffusion likely plays a key role in molecular signaling across the osteochondral interface. Some earlier studies on OA models of rabbits and rats reported the diffusion at the osteochondral interface (Weinans et al., 2012). The diffusion of small molecules ( < 400 Da) was confirmed between the uncalcified and calcified cartilage in the metacarpophalangeal joints of healthy mature horses (Arkill and Winlove, 2008). Diffusion of small molecules across the osteochondral interface in a murine model using sodium fluorescein (376 Da) was correlated with OA progression and diffusion of Gd-DTPA$^{2-}$ (MRI contrast agent, 547 Da) in the clinic was observed (Burstein et al., 2001; Pan et al., 2009b, 2012). The presence of non-mineralized patches (~100 nm) within the calcified cartilage as well as invasion of

* Corresponding author at: Department of Orthopedics, UMC Utrecht, Heidelberglaan 100, 3584 CX Utrecht, The Netherlands.
*E-mail addresses:* b.pouran-2@umcutrecht.nl, b.pouran@gmail.com (B. Pouran).

http://dx.doi.org/10.1016/j.jbiomech.2016.12.025
0021-9290/© 2017 Elsevier Ltd. All rights reserved.

uncalcified cartilage through the calcified cartilage might explain the molecular transport (Pan et al., 2009a; Lyons et al., 2006). Unlike articular cartilage, consensus exists regarding the diffusion

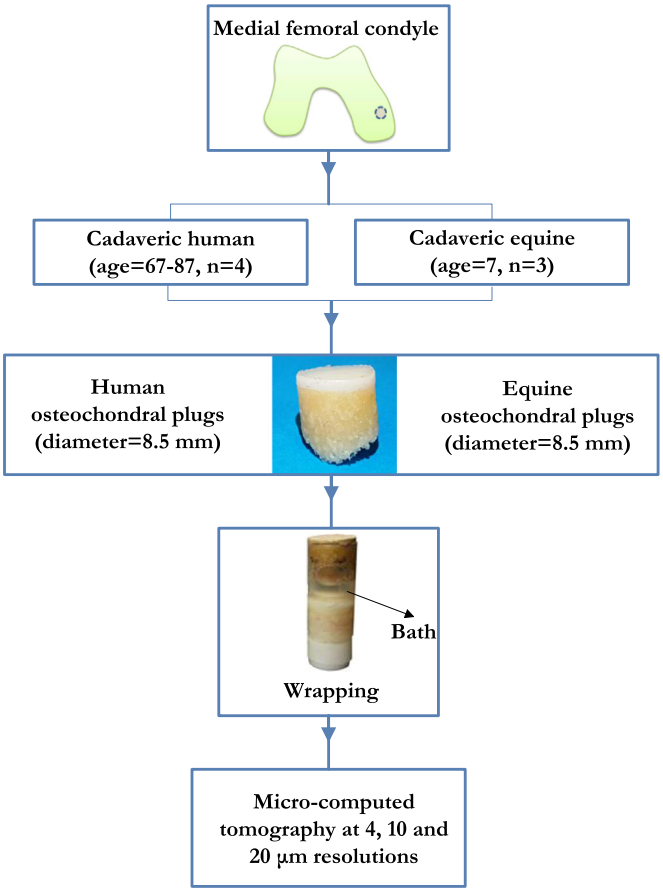


**Fig. 1.** Preparing samples for the micro-CT scanning: osteochondral plugs were extracted from four cadaveric human medial femoral condyles and three cadaveric equine medial femoral condyles. A shrinking sleeve was used to wrap the samples before injecting the contrast agent onto the cartilage surface. Then the samples underwent multi-resolution micro-computed tomography.

of molecules between the intervertebral disk (IVD) and the vertebral body through the endplate. Diffusion is known to dramatically influence the health of the spine, because insufficient nutrition of the IVD is suggested to accelerate its degeneration (Galbusera et al., 2014). However, it was shown that load-dependent convection facilitates the transport in the IVD as well as across the endplate-IVD interface in both healthy and degenerated disks (Gullbrand et al., 2015a, 2015b). A previous study using advanced micro-computed tomography (micro-CT) showed increased perforations in the subchondral endplate when the IVD degenerates (Rutges et al., 2011). All the previous evidence therefore supports the theory that direct diffusion between cartilaginous tissues and underlying bone plays a key role in the normal physiology of articulating joints as well as the spine.

In the present study, we aim to investigate solute transport between articular cartilage and subchondral bone of equine and human samples using multi-resolution micro-CT by applying a neutral solute. Using the neutral solute enables to exclude the mechano-electrical phenomena arising when an external charged solute is transferred through the highly charged articular cartilage. The effects of the micro-architecture (i.e. porosity and thickness) of the calcified cartilage/subchondral bone plate complex and thickness of uncalcified cartilage on diffusion will be determined.

## 2. Methodology

### 2.1. Experiments

#### 2.1.1. Bath and sample preparation

The criterion for OA detection was based on visual observations performed by two surgeons and one engineer: regions where the cartilage has completely disappeared were considered as advanced OA, whereas, regions with existing cartilage but having relatively rough surface were considered as slight OA. Cylindrical osteochondral plugs from four cadaveric fresh-frozen human medial femoral condyles with slight OA (approved by university medical center Utrecht, age=67–85, $n_{total}=4$, cartilage thickness=2.53 ± 0.31 mm, diameter=8.5 mm) and three healthy cadaveric equine medial femoral condyles (approved by Utrecht university,

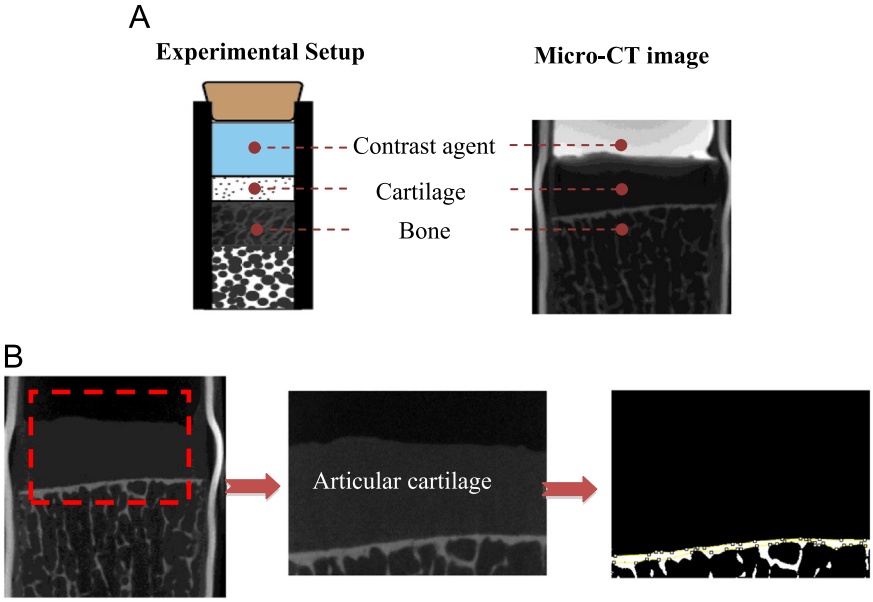


**Fig. 2.** Micro-computed tomography image with spatial resolution of 20 $\mu m^3$ (A). Local thresholding was employed before injection of contrast agent to calculate the thickness and porosity of the subchondral bone plate/calcified cartilage (B).

**Table 1**
Cartilage thickness, subchondral plate/calcified cartilage thickness and porosity for human samples (4 donors) and for equine samples (3 donors).

| Sample | | Cartilage thickness (μm) | Subchondral plate/ calcified cartilage thickness (μm) | Subchondral plate/ calcified cartilage porosity (%) |
|---|---|---|---|---|
| Human | 1 | 2500 | 175 | 4.8 |
| | 2 | 2700 | 115 | 6.4 |
| | 3 | 2100 | 186 | 4.0 |
| | 4 | 2800 | 147 | 8.1 |
| Equine (donor 1) | 1 | 700 | 178 | 12.1 |
| | 2 | 1100 | 468 | 7.6 |
| | 3 | 830 | 117 | 17.2 |
| | 4 | 1320 | 193 | 5.1 |
| | 5 | 1190 | 175 | 3.5 |
| | 6 | 2100 | 332 | 1.5 |
| Equine (donor 2) | 1 | 1800 | 115 | 6 |
| | 2 | 1300 | 153 | 10 |
| | 3 | 1108 | 112 | 6.1 |
| | 4 | 1228 | 427 | 2.8 |
| | 5 | 2560 | 738 | 3 |
| Equine (donor 3) | 1 | 900 | 235 | 2 |
| | 2 | 1611 | 350 | 7.5 |
| | 3 | 1800 | 545 | 3.2 |
| | 4 | 1240 | 525 | 4.9 |
| | 5 | 2246 | 850 | 1.5 |
| | 6 | 2070 | 900 | 1 |

age=7, $n_{total}$=17, cartilage thickness=1.48 ± 0.53 mm, diameter=8.5 mm) were drilled using custom-made drill bits (Fig. 1). For the human samples, care was taken to extract them from a location that was visually intact. The site of drilling was constantly sprayed using phosphate buffer serum (PBS) to ensure minimal dehydration and damage to the cartilage.

We prepared iodixanol solutions (molecular weight (MW)= 1.55 kDa, concentration=420 mM, charge=0, osmolality=300 mOsm/kg$H_2O$, volume ≃ 600 μL, GE Healthcare, *Netherlands*) enriched with protease inhibitors (5 mM, cOmplete, Roche, *Germany*) to study the axial diffusion through cartilage and the cartilage-bone interface. Since iodixanol is a neutral contrast agent, the effect of cartilage charge on molecular transport was eliminated. Immediately post-harvest, the osteochondral plugs were wrapped using plastic shrinking sleeves to prevent lateral diffusion (Fig. 1).

### 2.1.2. Quantitative micro-CT

To study the transport of iodixanol across cartilage and the cartilage-bone interface, we used a micro-CT scanner (*Quantum FX*, Perkin Elmer, USA, spatial resolution of 20 $\mu m^3$ voxel size, scan time=3 min, tube voltage=90 kV and tube current=180 μA, number of projections=3600) and captured images at $t_{-1}$ (before injection of iodixanol solution), $t_0$ (point of injection of iodixanol solution), $t$=12, 24, 48 and 72 h within the field of views consisting of bath, cartilage, and subchondral bone (Fig. 2A).

The projected images were transformed automatically to 3D reconstructed files using in-built software of the micro-CT machine (*Quantum FX*). After rigid image registration based on the $t_0$ images, the 3D reconstructed files were converted to a series of 2D images for further analyses (*Analyze 11.0*). We used Gaussian blurring 3D filter (radius=3) to minimize the noise and then selected 20 middle slices of the 2D stack and created rectangular regions of interest (ROI) in *FIJI (free software for image analyses)*, which comprised the bath, cartilage, and subchondral plate. The $t_{-1}$ images were locally thresholded (*Bernsen*) and *BoneJ* (plugin of *FIJI*) was used to calculate the thickness and porosity of the subchondral plate/calcified cartilage as well as the thickness of uncalcified cartilage (Fig. 2B and Table 1). The subchondral plate/calcified cartilage zone was defined as the region lying above the region where the trabecular structure could be easily pinpointed. The mean of the average grey values of the subchondral plate/calcified cartilage at $t_0$ in 20 selected slices was subtracted from the mean average grey values at the later time points to measure the diffusion. The relationship between the diffusion at 72 h with the micro-architecture of subchondral plate/calcified cartilage, i.e. porosity and thickness, was also investigated.

### 2.1.3. Qualitative micro-CT

To qualitatively visualize the diffusion at the cartilage-bone interface we also performed micro-CT scan using the previously mentioned micro-CT parameters but with higher spatial resolution of 10 $\mu m^3$. To visualize the cartilage-bone interface, ultra-high-resolution *phoenix nanotom* micro-CT was used (GE, USA, tube voltage=70 kV tube current=110 μA, 4 $\mu m^3$ voxel size, scan time=2 h, field of view: 4 mm).

## 3. Results

The thickness of cartilage for human and equine samples was 2525 ± 310 μm and 1476 ± 537 μm, respectively. For human samples the thickness and porosity of the subchondral plate were 155.7 ± 31.3 μm and 5.8 ± 1.8% and for equine samples the thickness and porosity of the subchondral plate were 377.2 ± 260.1 μm and 5.6 ± 4.3% (Table 1).

Diffusion of iodixanol from uncalcified cartilage to the subchondral bone via the calcified cartilage layer for both the human and equine samples was confirmed (Figs. 3 and 4). Low cartilage thickness, high subchondral plate/calcified cartilage porosity and low subchondral plate/calcified cartilage thickness are factors contributing to diffusion (Table 1, Fig. 5A and B). In the human samples, we observed the steepest rise in the diffusion within the subchondral plate/calcified cartilage until $t$=24 h (Fig. 5A). After 24 h, the diffusion curves tended to reach near-equilibrium, achieving the highest average grey value at 72 h. For all time points, the average grey values were the highest in sample 2 (human), which has the lowest thickness of the subchondral plate/calcified cartilage (Fig. 5A and Table 1). Samples 1 and 3 (human) showed diffusion patterns that were very similar to each other (Fig. 5A), as well as similar morphological characteristics (Table 1). Like the observations regarding human samples, the diffusion curves in the equine samples reach near-equilibrium at 72 h (Fig. 5B).

Plots of near-equilibrium increase in average grey values versus morphological features (porosity and thickness) of the subchondral plate/calcified cartilage for both equine and human samples suggested a link between diffusion behavior of the neutral solute and the micro-architecture of the subchondral plate/calcified cartilage (Fig. 6). To investigate the relationship of cartilage thickness and subchondral plate/calcified thickness and porosity on diffusion we performed multi-regression analysis. This analysis was not possible to perform on human samples due to relatively low sample number. Multi-regression on equine samples showed strong correlation (multiple $R$=0.97) with significance of porosity ($p$-value < 5e-7) and thickness ($p$-value < 0.05) of subchondral plate/calcified cartilage on diffusion. Diffusion in human samples did not correlate with porosity as compared to equine samples (Fig. 6A, $R^2$=0.24 vs. $R^2$=0.90). Nevertheless, diffusion in the human samples had a stronger correlation with the thickness of subchondral plate/calcified cartilage compared to equine samples (Fig. 6B, $R^2$=0.92 vs. $R^2$=0.50).

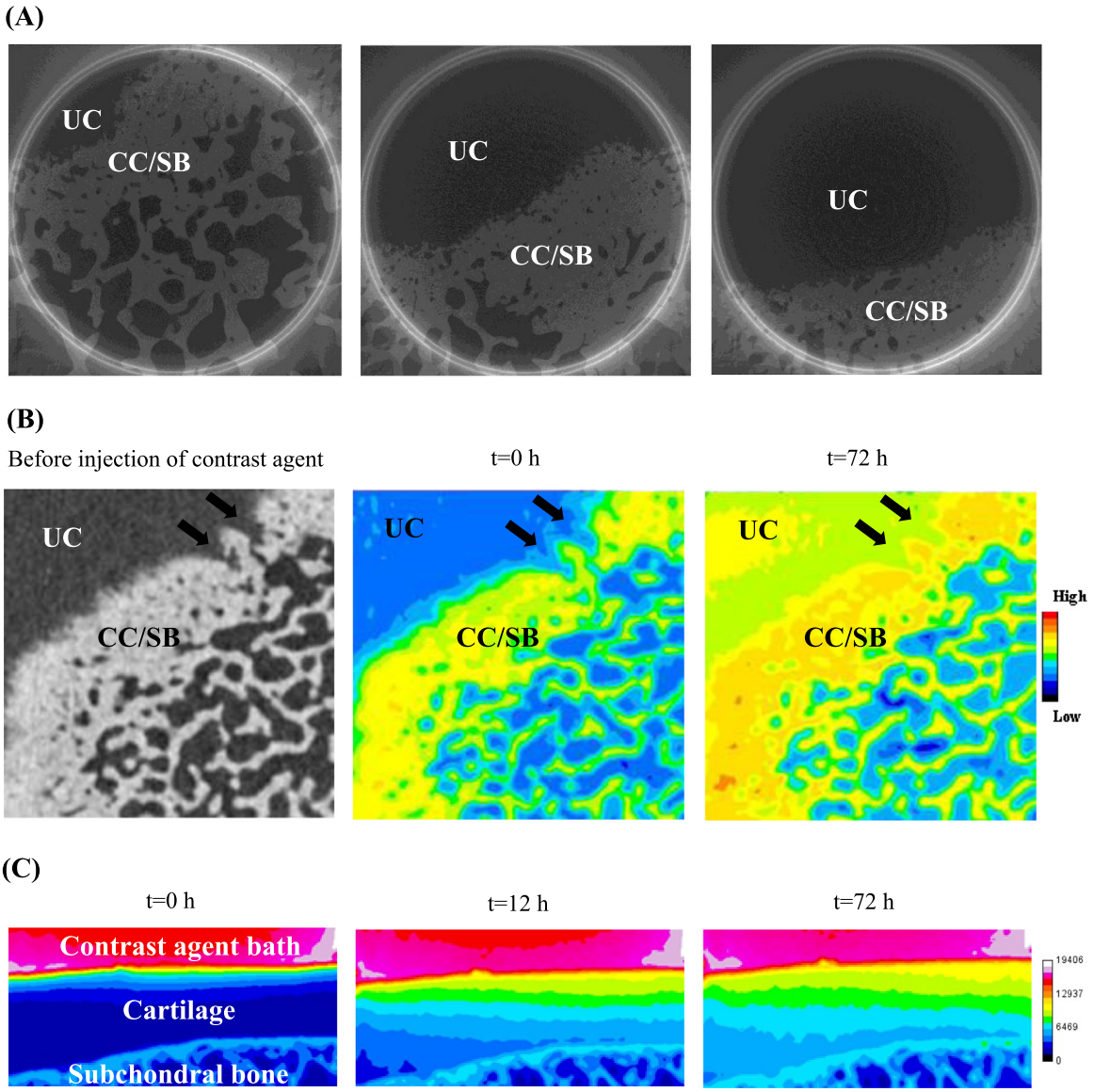


**Fig. 3.** Ultra-high micro-CT (4 $\mu m^3$ spatial resolution) was used to highlight the interface of cartilage and subchondral bone plate in three representative slices in a human osteochondral plug. The diffusion at the interface of uncalcified cartilage (UC) and subchondral bone plate (SB)/calcified cartilage (CC) is depicted (A). The protrusion of uncalcified cartilage into the calcified cartilage and mineralized region (arrows) facilitates the diffusion (10 $\mu m^3$ spatial resolution) (B). The progress of the diffusion front wave is shown at different time points (20 $\mu m^3$ spatial resolution) (C).

## 4. Discussion

In this study, we have observed the direct diffusion between articular cartilage and subchondral bone plate/calcified cartilage in human as well as equine osteochondral plugs when a finite volume of baths containing a neutral solute was inserted at the cartilage surface. Furthermore, we confirmed that the molecular transport to the subchondral bone plate depends on the morphological parameters of both uncalcified cartilage and subchondral bone plate. We identified cartilage thickness and thickness as well as porosity of subchondral bone plate as the factors influencing the transport. Porosity and thickness of the subchondral plate in horse samples were found to have more effect on the diffusion across osteochondral interface compared to cartilage thickness. In equine samples, porosity of subchondral plate/calcified cartilage revealed stronger effect on diffusion than thickness of subchondral plate/calcified cartilage (Fig. 6). In human samples, small variation in subchondral plate porosity was observed and the effect of subchondral plate thickness on diffusion was more tangible (Fig. 6).

The electrically neutral molecules (MW = 1.55 kDa) used in our study allowed excluding the effects of fixed charges entrapped in the articular cartilage and the resulting electro-mechanically induced transport. Therefore, in the current study molecular friction between the diffusing solute and the extracellular matrix of the cartilage, i.e. water content, collagen fibrils and proteoglycans as well as the morphology of subchondral plate (porosity and thickness) are the only limiting factors for neutral molecular transport between cartilage and underlying bone. This implies that the diffusion mechanism in our study can be described as a Fickian diffusion process (Pouran et al., 2016). In samples with similar thickness of the articular cartilage, we observed higher near-equilibrium increase in average grey value (diffusion, 72 h) (Fig. 5A), which is likely due to the thinner subchondral plate/calcified cartilage (28% difference, Table 1). Similar diffusion behavior in human samples before 12 h (Fig. 5A) may be linked to the fact that similar cartilage thicknesses could lead to similar

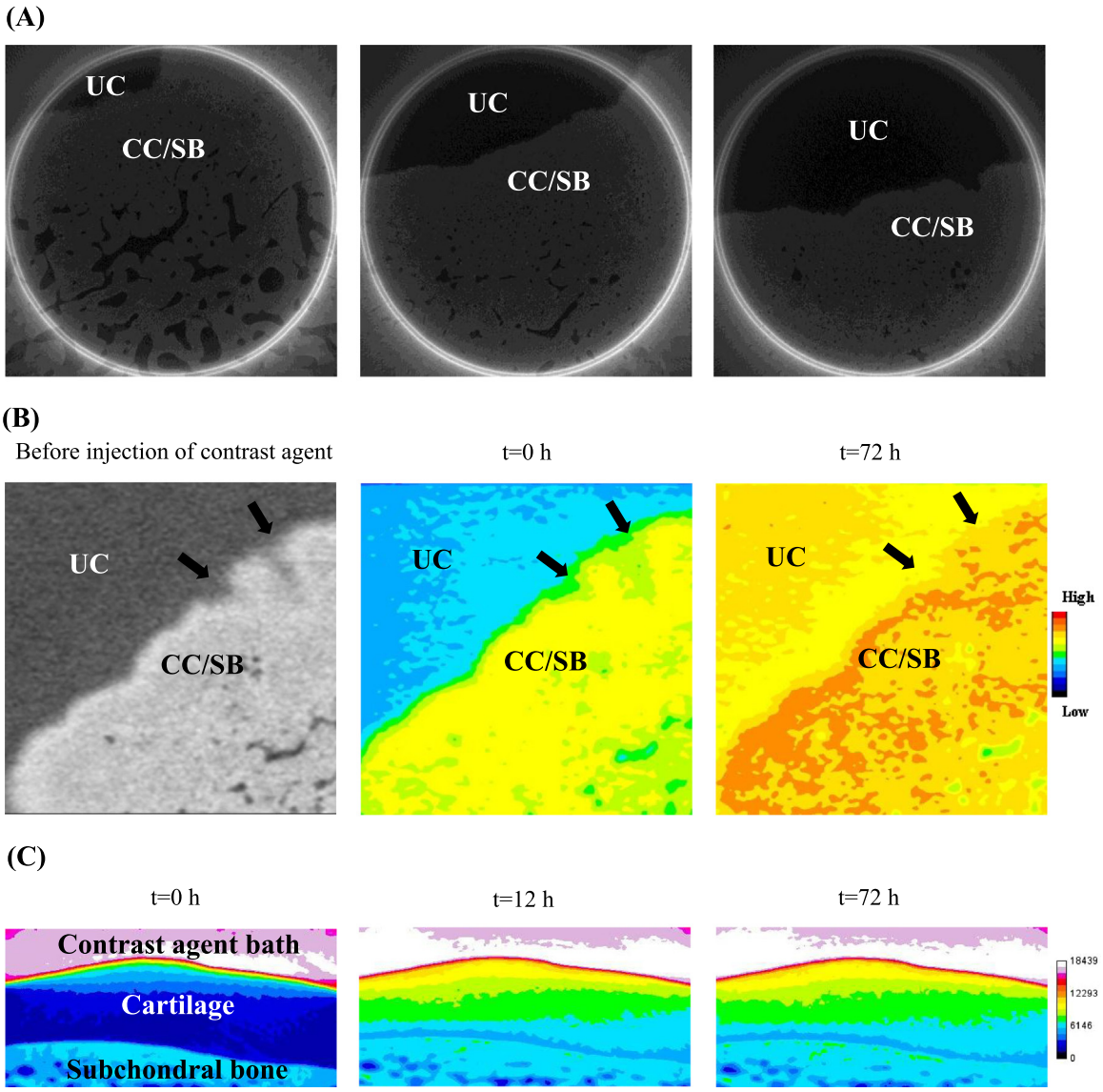


**Fig. 4.** Ultra-high micro-CT (4 $\mu m^3$ spatial resolution) was used to highlight the interface of cartilage and subchondral bone plate in three representative slices in an equine osteochondral plug. The diffusion at the interface of uncalcified cartilage (UC) and subchondral bone plate (SB)/calcified cartilage (CC) is depicted (A). The protrusion of uncalcified cartilage into the calcified cartilage and mineralized region (arrows) facilitates the diffusion (10 $\mu m^3$ spatial resolution) (B). The progress of the diffusion front wave is shown at different time points (20 $\mu m^3$ spatial resolution) (C).

frictional loss in driving force eventually causing similar diffusion behavior in the subchondral plate/calcified cartilage (Table 1).

The structural changes such as thinning of the subchondral plate in early OA (Botter et al., 2011; Intema et al., 2010a) and subchondral bone sclerosis observed in advanced OA may alter the transport rate causing interruptions in trans-signaling between cartilage and subchondral bone plate. Our study also emphasizes the importance of structure of the subchondral bone on the transport across osteochondral interface. Human samples that represent similar thickness and porosity of the subchondral plate/calcified cartilage showed very similar diffusion behavior in all time points (Fig. 5A and Table 1). Enhanced porosity creates more access for the solutes to diffuse across the subchondral plate since the pores filled with soft tissue with high water content are more permeable than the mineralized regions of subchondral plate. A previous study on murine model of OA also suggested that the transport between cartilage and subchondral plate increases due to thinning of cartilage and subchondral plate (Pan et al., 2012), which is in agreement with our observations. It should be borne in mind that the inter-connectivity and tortuosity of the pores has not been investigated in this study, but could themselves play an integral role in solutes distribution and partitioning. Since both young (equine) and old and perhaps slightly OA joints (human) were used in this study we can draw the conclusion that the interface of cartilage and subchondral bone plate is permeable to at least relatively small solutes (less than 2 kDa) in both healthy and slightly degenerated joints. To our best of knowledge, we were the first who investigated the transport of relatively larger solutes across osteochondral interface compared to other previous studies (Arkill and Winlove, 2008; Burstein et al., 2001) in both human and horse knees taking the morphology of the cartilage and bone into account.

Whereas the current study strived to be as thorough as possible, it is inevitably associated with some limitations. First, the calcified cartilage and subchondral plate could not be differentiated clearly from each other using micro-CT images, especially when the contrast agent (iodixanol) diffused through them which limited the capability of studying the diffusion separately in these

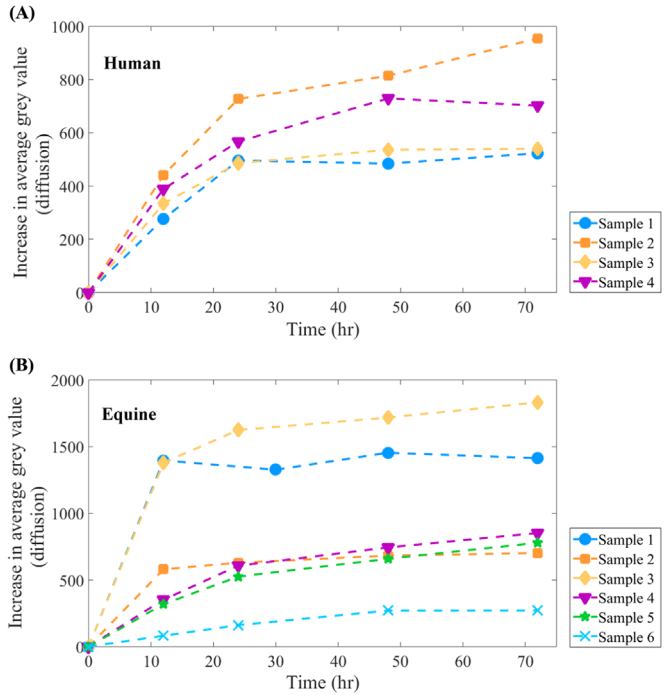


**Fig. 5.** Average grey values (diffusion) in the subchondral plate/calcified cartilage over-time for human (A) and for equine samples (donor 1) as the representative data (B).

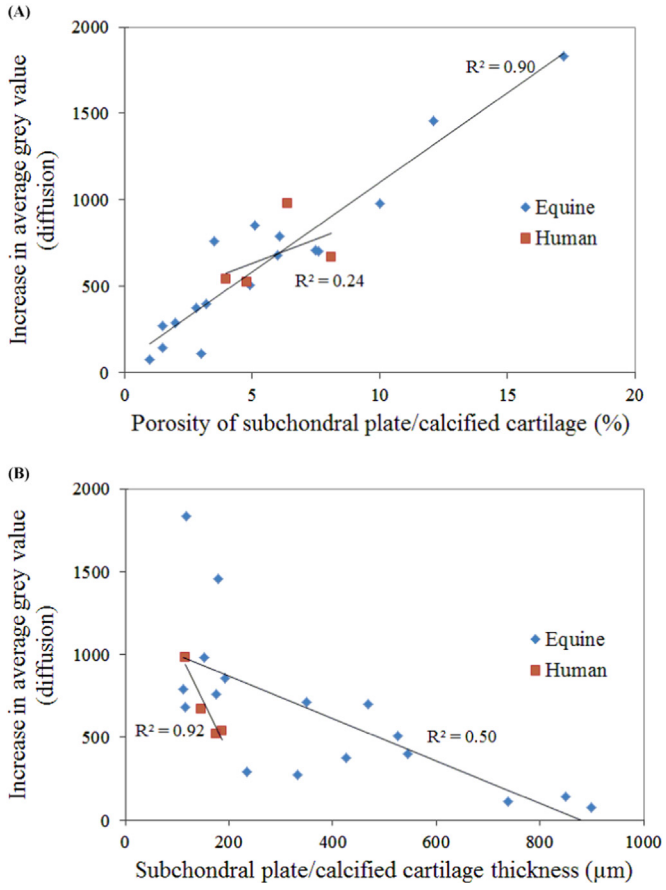


**Fig. 6.** Plot of average grey values (diffusion) at 72 h in the subchondral plate/calcified cartilage versus subchondral plate/calcified cartilage porosity (A) and subchondral plate/calcified cartilage thickness (B).

two zones. Second, although our study used largest solute among the similar studies and applied it in large animal model and human, the diffusion of vital signaling macromolecules may be studied by labeling them with contrast agents using synthetic molecular assembly techniques. Furthermore, the effect of solute charge on diffusion in the subchondral plate/calcified cartilage could be investigated in future studies to enable studying charged signaling molecule transfer across the osteochondral interface.

The present study sheds light on the transport of a neutral solute across the interface of articular cartilage and subchondral plate. Our findings confirm the direct cross-talk between cartilage and subchondral bone/calcified cartilage in both human samples (slightly osteoarthritic) and equine samples (healthy) when applying a neutral contrast agent to nullify the mechano-electrical-affected diffusion in the articular cartilage. Besides, we highlighted that diffusion in the subchondral plate/calcified cartilage could be estimated when micro-architecture data concerning porosity and thickness of the subchondral plate/calcified cartilage and cartilage thickness are available.

## Conflicts of interest

Authors have no conflicts of interest.

## Acknowledgements

This work was supported by a Grant from Dutch Arthritis Foundation (LRP-22). The authors are grateful to Mr. Michael Afanasyev and Mr. Wim Verwaal for their assistance during high-resolution micro-CT scans.

## References

Arkill, K.P., Winlove, C.P., 2008. Solute transport in the deep and calcified zones of articular cartilage. Osteoarthr. Cartil. 16, 708–714.

Botter, S.M., 2010. Dynamic Subchondral Bone Changes in Murine Models of Osteoarthritis (Ph.D. thesis).

Botter, S.M., van Osch, G.J., Clockaerts, S., Waarsing, J.H., Weinans, H., van Leeuwen, J.P., 2011. Osteoarthritis induction leads to early and temporal subchondral plate porosity in the tibial plateau of mice: an in vivo microfocal computed tomography study. Arthritis Rheum. 63, 2690–2699.

Burstein, D., Velyvis, J., Scott, K.T., Stock, K.W., Kim, Y.-J., Jaramillo, D., Boutin, R.D., Gray, M.L., 2001. Protocol issues for delayed Gd(DTPA)2--enhanced MRI (dGEMRIC) for clinical evaluation of articular cartilage. Magn. Reson. Med. 45, 36–41.

Galbusera, F., Brayda-Bruno, M., Wilke, H.J., 2014. Is post-contrast MRI a valuable method for the study of the nutrition of the intervertebral disc? J. Biomech. 47, 3028–3034.

Gullbrand, S.E., Peterson, J., Ahlborn, J., Mastropolo, R., Fricker, A., Roberts, T.T., Abousayed, M., Lawrence, J.P., Glennon, J.C., Ledet, E.H., 2015a. ISSLS prize winner: dynamic Loading-induced convective transport enhances intervertebral disc nutrition. Spine 40, 1158–1164.

Gullbrand, S.E., Peterson, J., Mastropolo, R., Roberts, T.T., Lawrence, J.P., Glennon, J.C., DiRisio, D.J., Ledet, E.H., 2015b. Low rate loading-induced convection enhances net transport into the intervertebral disc in vivo. Spine J.: Off. J. North Am. Spine Soc. 15, 1028–1033.

Intema, F., Hazewinkel, H.A., Gouwens, D., Bijlsma, J.W., Weinans, H., Lafeber, F.P., Mastbergen, S.C., 2010a. In early OA, thinning of the subchondral plate is directly related to cartilage damage: results from a canine ACLT-meniscectomy model. Osteoarthr. Cartil. 18, 691–698.

Intema, F., Sniekers, Y.H., Weinans, H., Vianen, M.E., Yocum, S.A., Zuurmond, A.M., DeGroot, J., Lafeber, F.P., Mastbergen, S.C., 2010b. Similarities and discrepancies in subchondral bone structure in two differently induced canine models of osteoarthritis. J. Bone Miner. Res. 25, 1650–1657.

Li, B., Aspden, R.M., 1997. Mechanical and material properties of the subchondral bone plate from the femoral head of patients with osteoarthritis or osteoporosis. Ann. Rheum. Dis. 56, 247–254.

Lyons, T.J., McClure, S.F., Stoddart, R.W., McClure, J., 2006. The normal human chondro-osseous junctional region: evidence for contact of uncalcified cartilage with subchondral bone and marrow spaces. BMC Musculoskelet. Disord. 7, 52.

Pan, J., Wang, B., Li, W., Zhou, X., Scherr, T., Yang, Y., Price, C., Wang, L., 2012. Elevated cross-talk between subchondral bone and cartilage in osteoarthritic joints. Bone 51, 212–217.

Pan, J., Zhou, X., Li, W., Novotny, J.E., Doty, S.B., Wang, L., 2009a. In situ measurement of transport between subchondral bone and articular cartilage. J. Orthop. Res.: Off. Publ. Orthop. Res. Soc. 27, 1347–1352.

Pouran, B., Arbabi, A., Zadpoor, A.A., Weinans, H., 2016. Isolated effects of external bath osmolality, solute concentration, and electrical charge on solute transport across articular cartilage. Med. Eng. Phys. 38, 1399–1407. http://dx.doi.org/10.1016/j.medengphy.2016.09.003.

Radin, E.L., Rose, R.M., 1986. Role of subchondral bone in the initiation and progression of cartilage damage. Clin. Orthop. Relat. Res., 34–40.

Rutges, J.P., Jagt van der, O.P., Oner, F.C., Verbout, A.J., Castelein, R.J., Kummer, J.A., Weinans, W.J., Creemers, L.B., Dhert, W.J., 2011. Micro-CT quantification of subchondral endplate changes in intervertebral disc degeneration. Osteoarthr. Cartil./OARS, Osteoarthr. Res. Soc. 19, 89–95.

Siebelt, M., Waarsing, J.H., Groen, H.C., Muller, C., Koelewijn, S.J., de Blois, E., Verhaar, J.A., de Jong, M., Weinans, H., 2014. Inhibited osteoclastic bone resorption through alendronate treatment in rats reduces severe osteoarthritis progression. Bone 66, 163–170.

Sniekers, Y.H., Intema, F., Lafeber, F.P., van Osch, G.J., van Leeuwen, J.P., Weinans, H., Mastbergen, S.C., 2008. A role for subchondral bone changes in the process of osteoarthritis; a micro-CT study of two canine models. BMC Musculoskelet. Disord. 9, 20.

Weinans, H., Siebelt, M., Agricola, R., Botter, S.M., Piscaer, T.M., Waarsing, J.H., 2012. Pathophysiology of peri-articular bone changes in osteoarthritis. Bone 51, 190–196.

Westacott, C., 2002. Interactions between subchondral bone and cartilage in OA. Cells from osteoarthritic bone can alter cartilage metabolism. J. Musculoskelet. Neuronal Interact. 2, 507–509.